Supplementary Data

Boron Nanosheets Boosting Solar Thermal Water Evaporation

Xin Stella Zhang, Shudi Mao, Jiashu Wang, Casey Onggowarsito, An Feng, Rui Han, Hanwen Liu, Guojin Zhang, Zhimei Xu, Limei Yang, Qiang Fu* and Zhenguo Huang*

School of Civil and Environmental Engineering, University of Technology Sydney, Ultimo, New South Wales 2007, Australia

1. Supplementary figures and tables

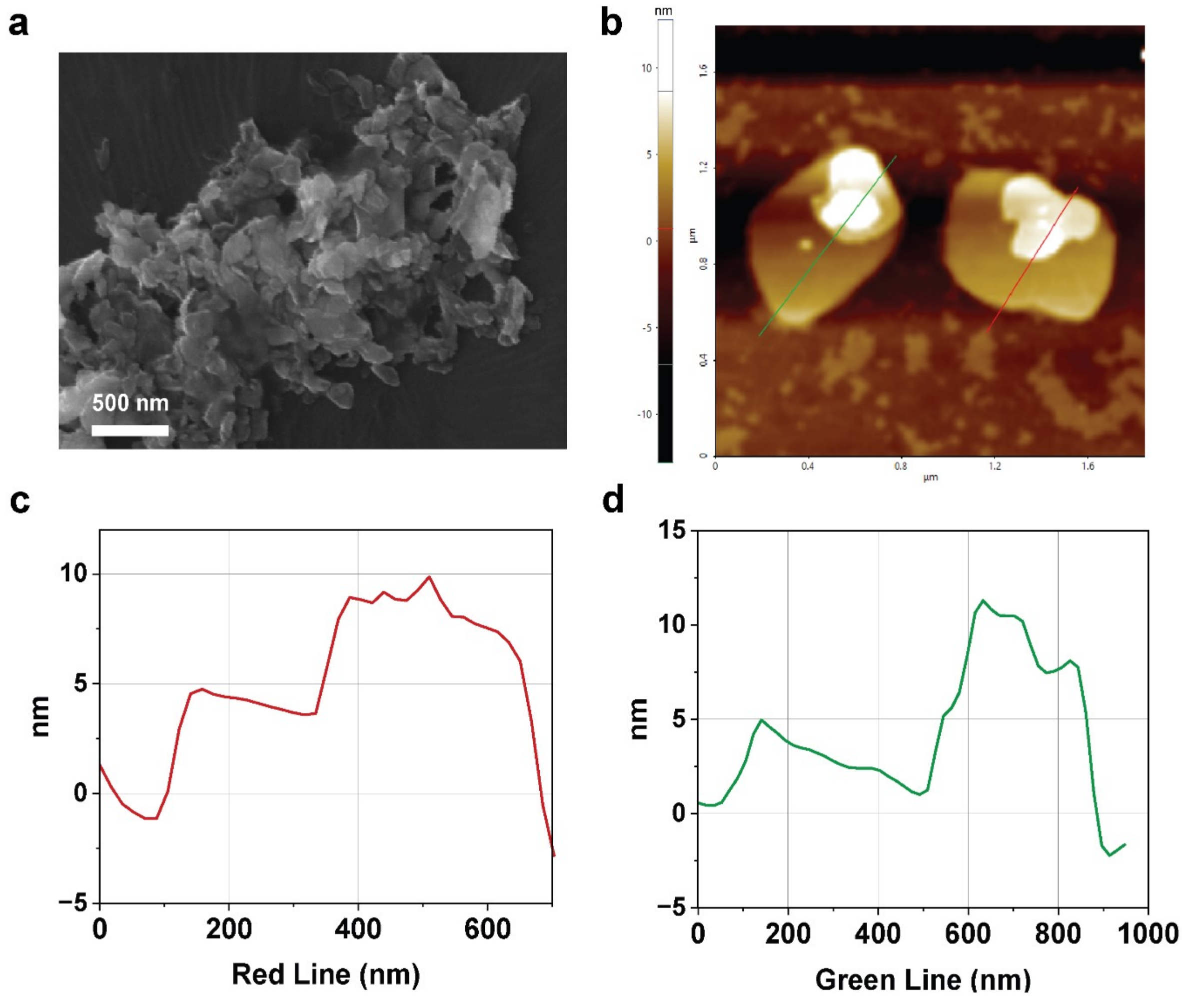

Fig. S1. (a) SEM image of CBNS, (b) AFM image of CBNS, (c-d) AFM analysis of CBNS showing the thickness of CBNS (green line and red line).

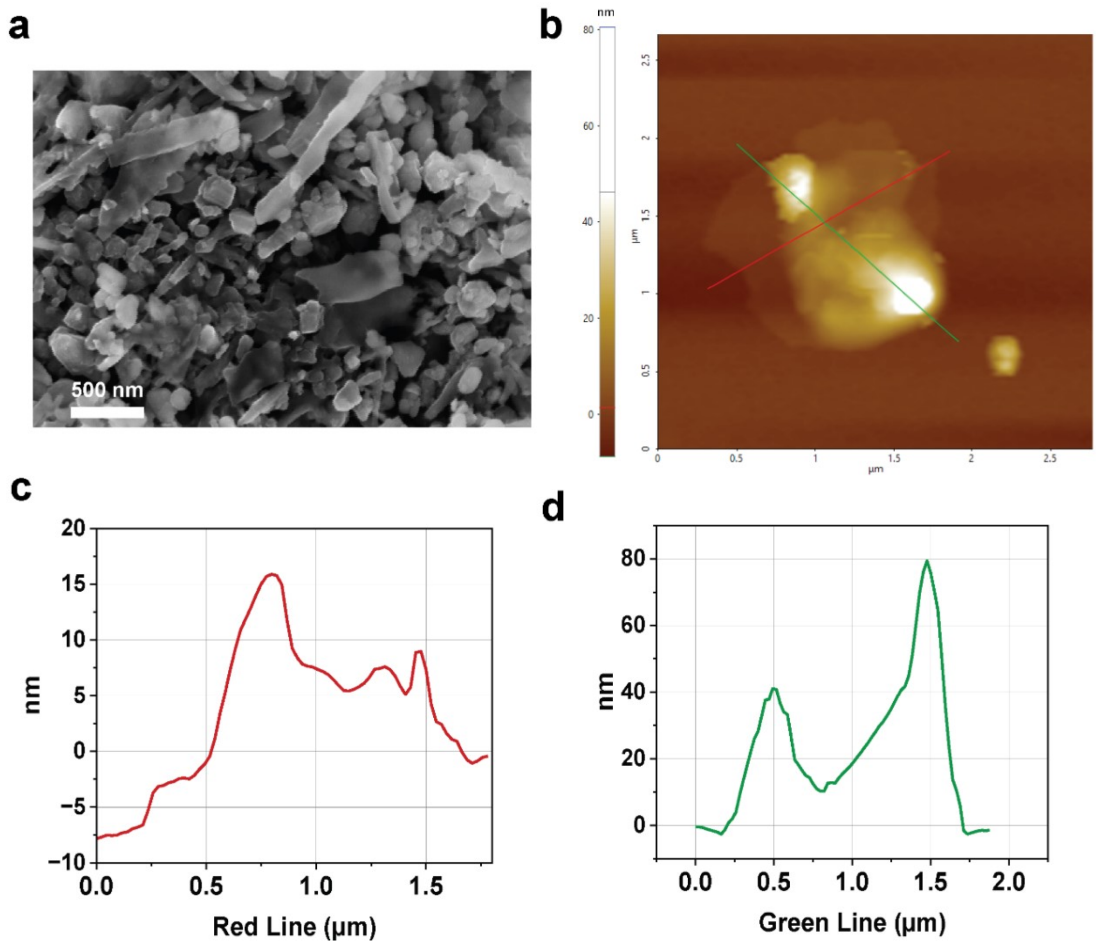

Fig. S2. (a) SEM image of ABNS, (b) AFM image of ABNS, (c-d) AFM analysis of ABNS showing the thickness of ABNS (green line and red line).

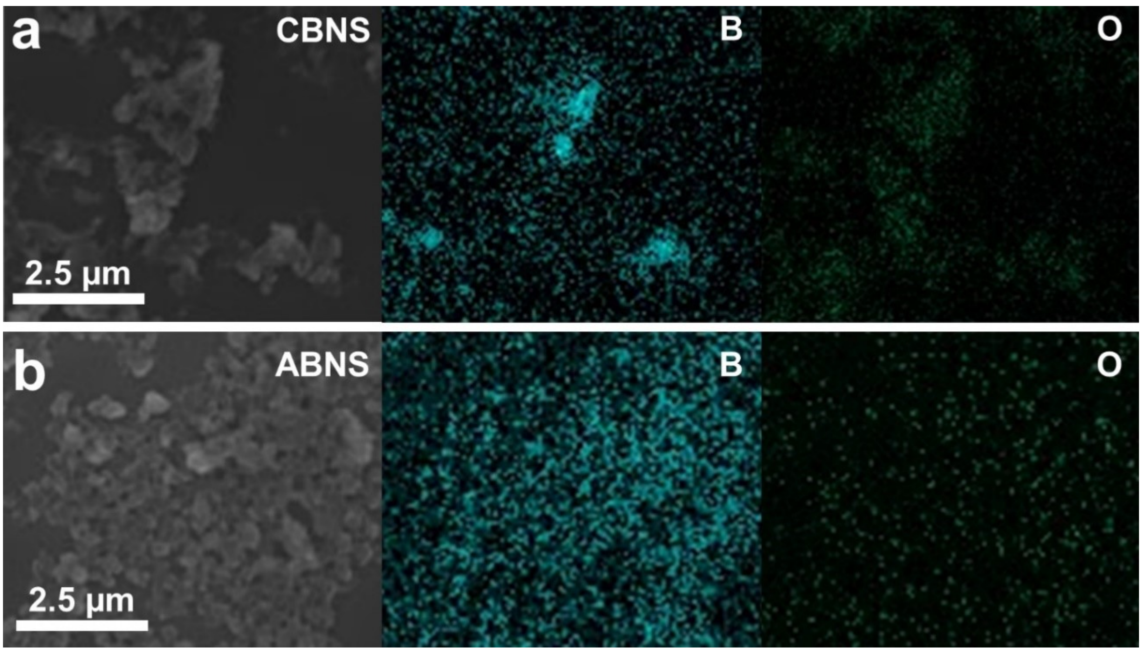

Fig. S3. Elemental mapping images of (a) CBNS and (b) ABNS.

X-ray photoelectron spectroscopy (XPS) data were calibrated using adventitious C1s peak at a fixed value of 284.4 eV.

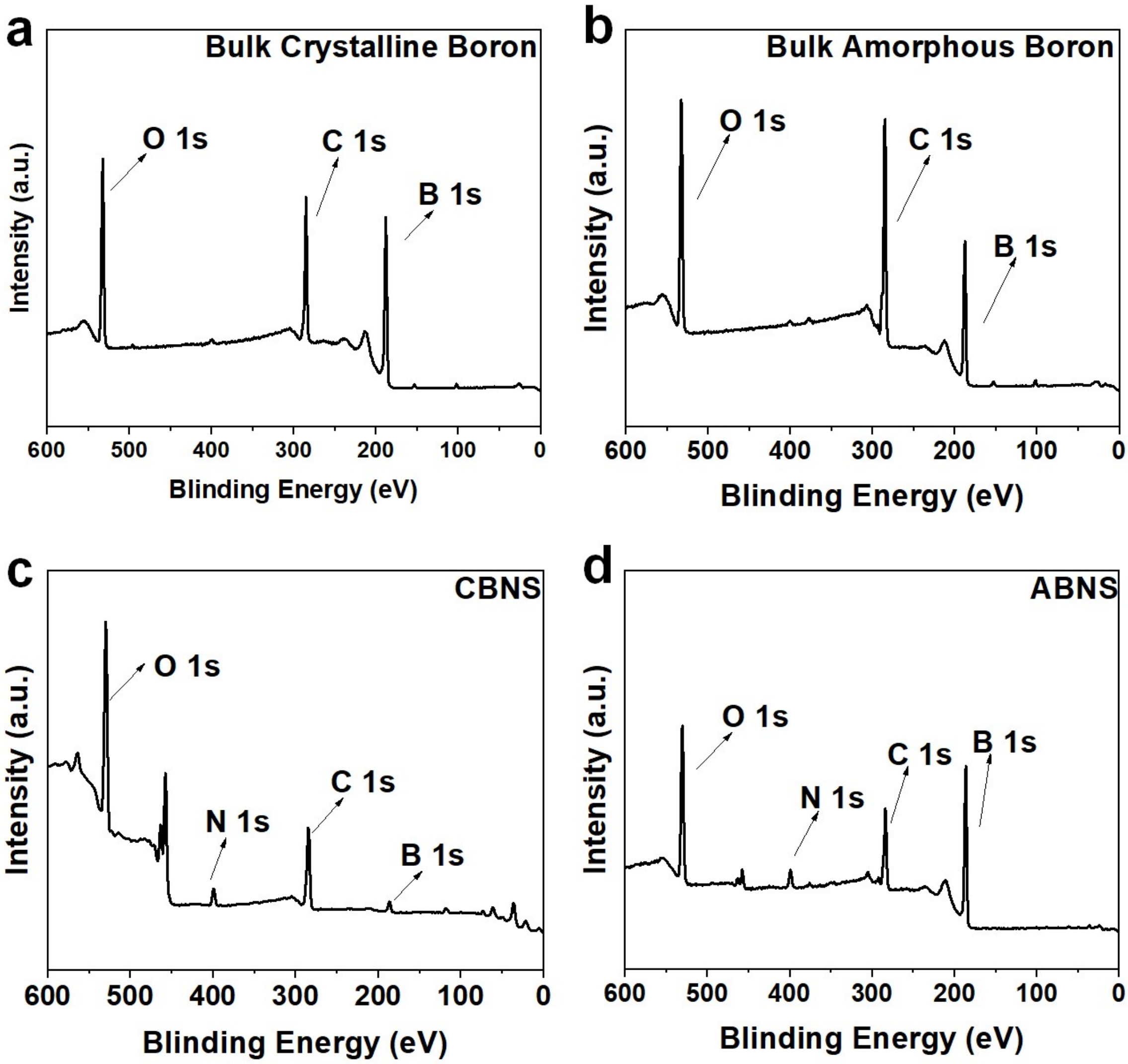

Fig. S4. Full-scale XPS survey spectra of (a) bulk crystalline boron, (b) bulk amorphous boron, (c) CBNS and (d) ABNS.

Table S1. The percentage of B-B and B-O bonds based upon the XPS spectra.

Samples	Ratio of bond peak	
	B-B	B-O
ABNS	82.26%	17.74%
Bulk Amorphous Boron	80.07%	19.93%
CBNS	74.75%	25.25%
Bulk Crystalline Boron	75.35%	24.65%

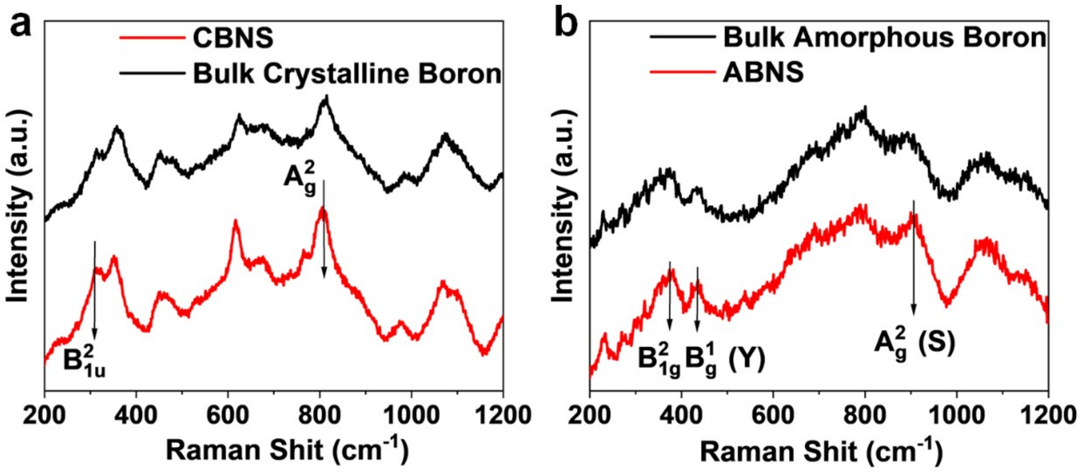

Fig. S5. Raman spectra of (a) CBNS and bulk crystalline boron, (b) ABNS and bulk amorphous Boron.

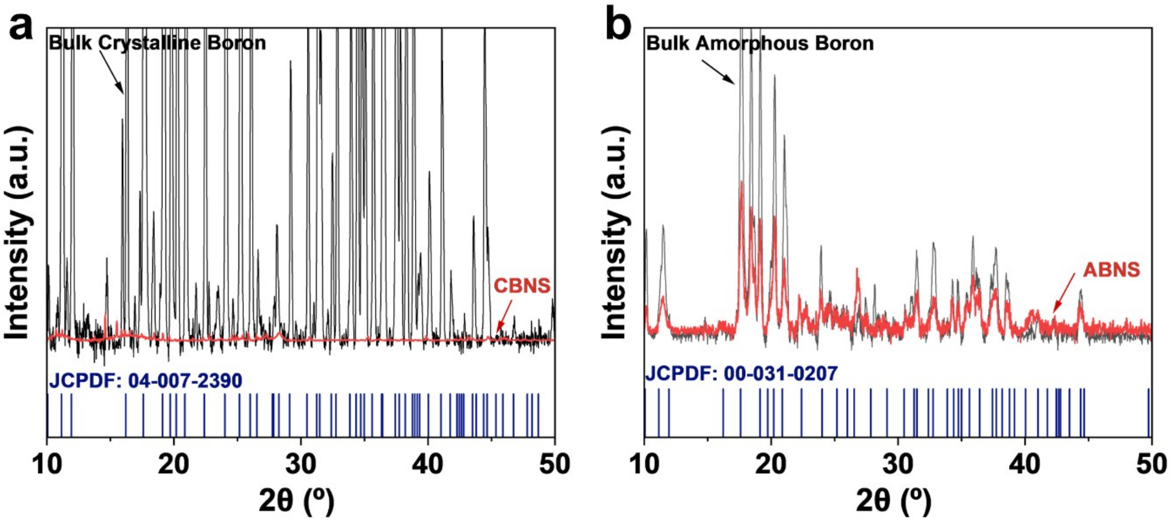

Fig. S6. XRD patterns of (a) bulk crystalline boron (JCPDF: 04-007-2390) and CBNS, (b) bulk amorphous boron (JCPDF: 00-031-0207-β-rhombohedral) and ABNS.

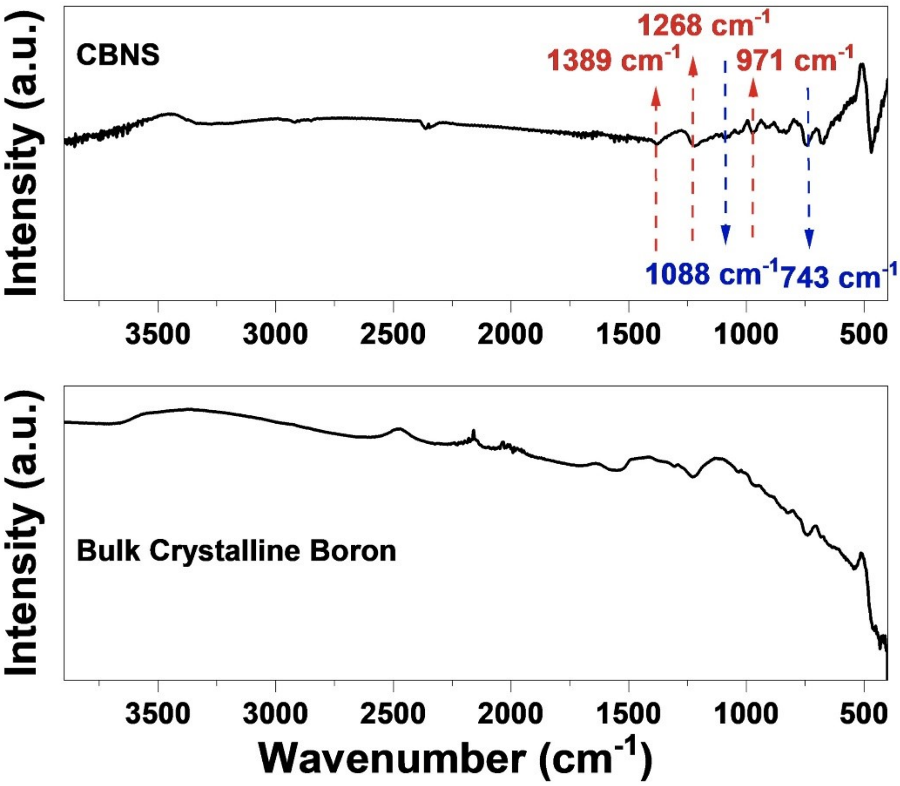

Fig. S7. FT-IR spectra of CBNS and bulk crystalline boron.

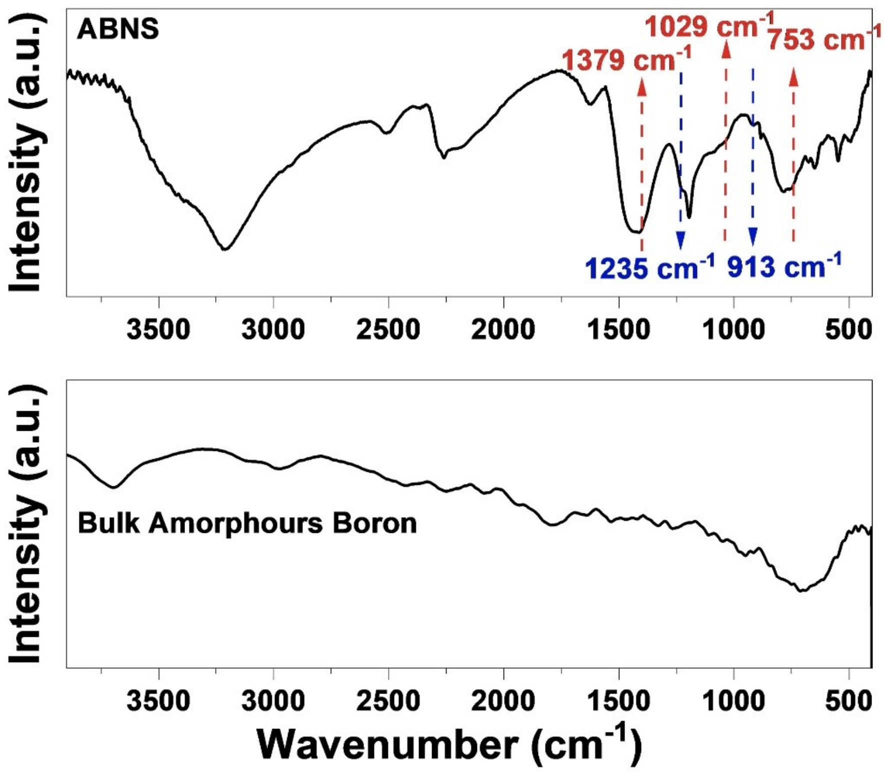

Fig. S8. FT-IR spectra of ABNS and bulk amorphous boron.

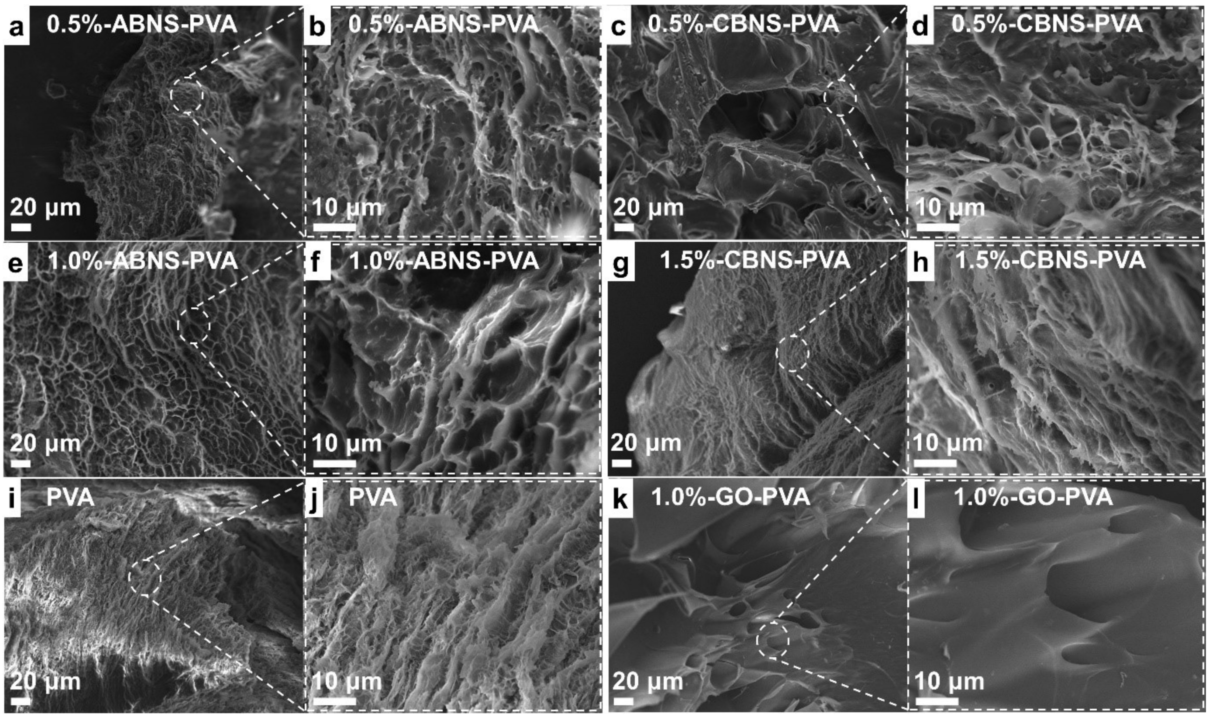

Fig. S9. SEM images of (a-b) 0.5%-ABNS-PVA, (c-d) 0.5%-CBNS-PVA, (e-f) 1.0%-ABNS-PVA, (g-h) 1.5%-CBNS-PVA PVA, (i-j) PVA, and (k-l) 1.0%-GO-PVA.

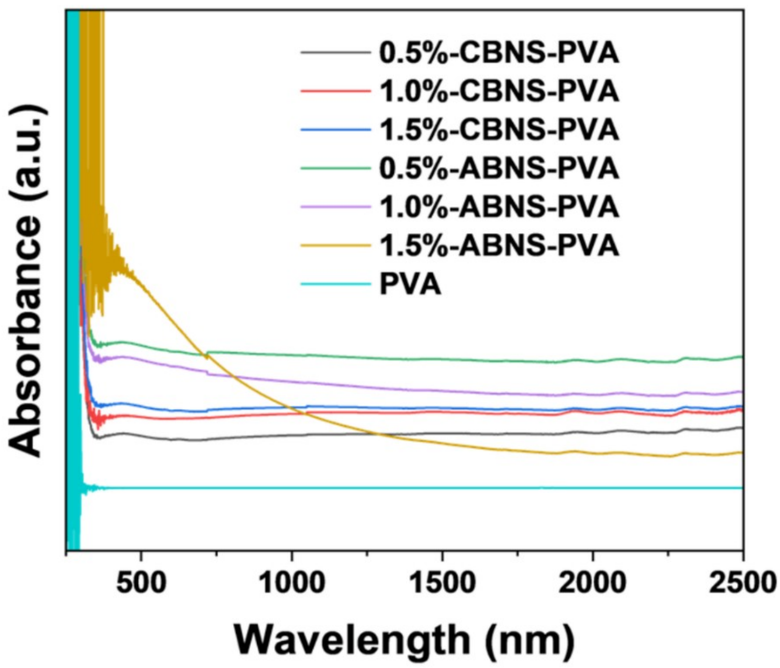

Fig. S10. UV-vis-NIR spectra of x-CBNS-PVA hydrogel and x-ABNS-PVA.

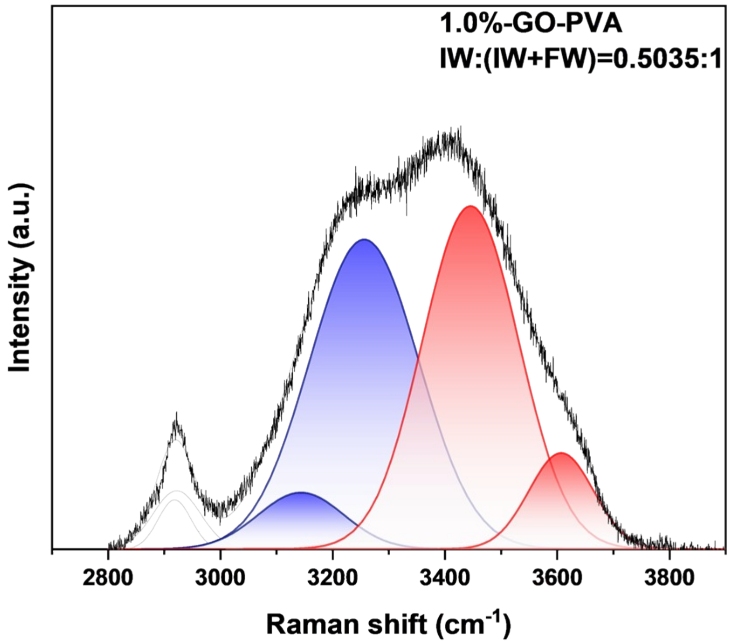

Fig. S11. Raman spectrum of 1.0%-GO-PVA shows the intermediate water content.

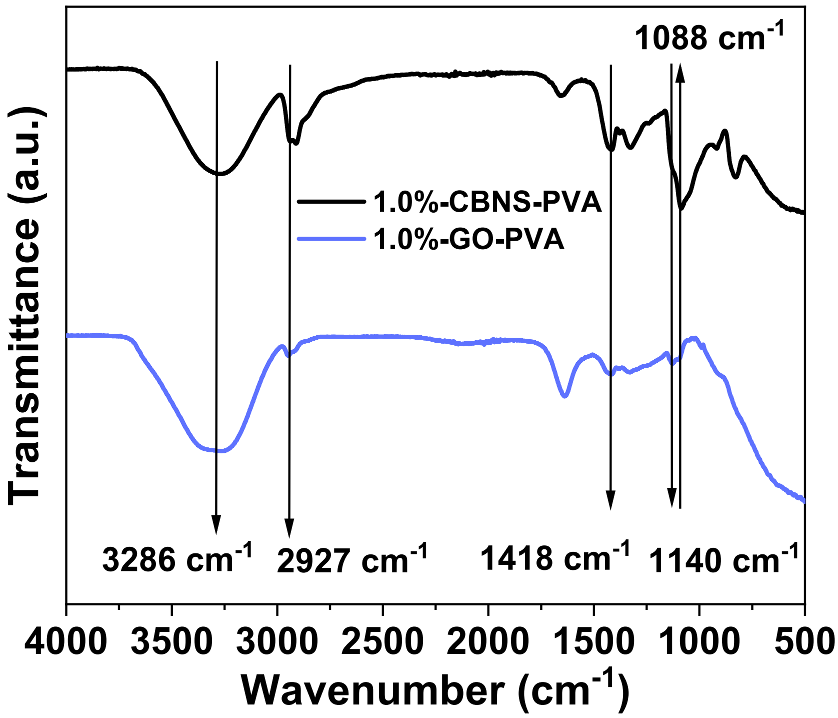

Fig. S12. FTIR spectra of 1.0%-CBNS-PVA (black line) and 1.0%-GO-PVA (blue line).

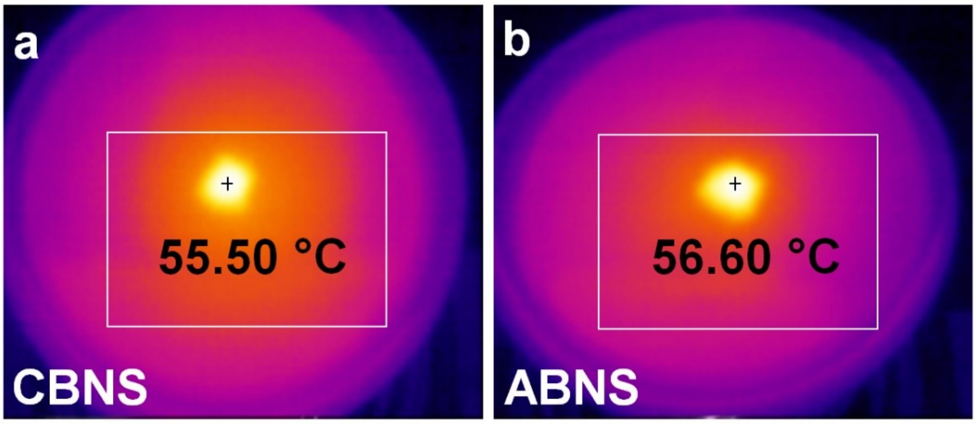

Fig. S13. Thermal infrared images of (a) CBNS and (b) ABNS powders under 1 sun after 60 mins

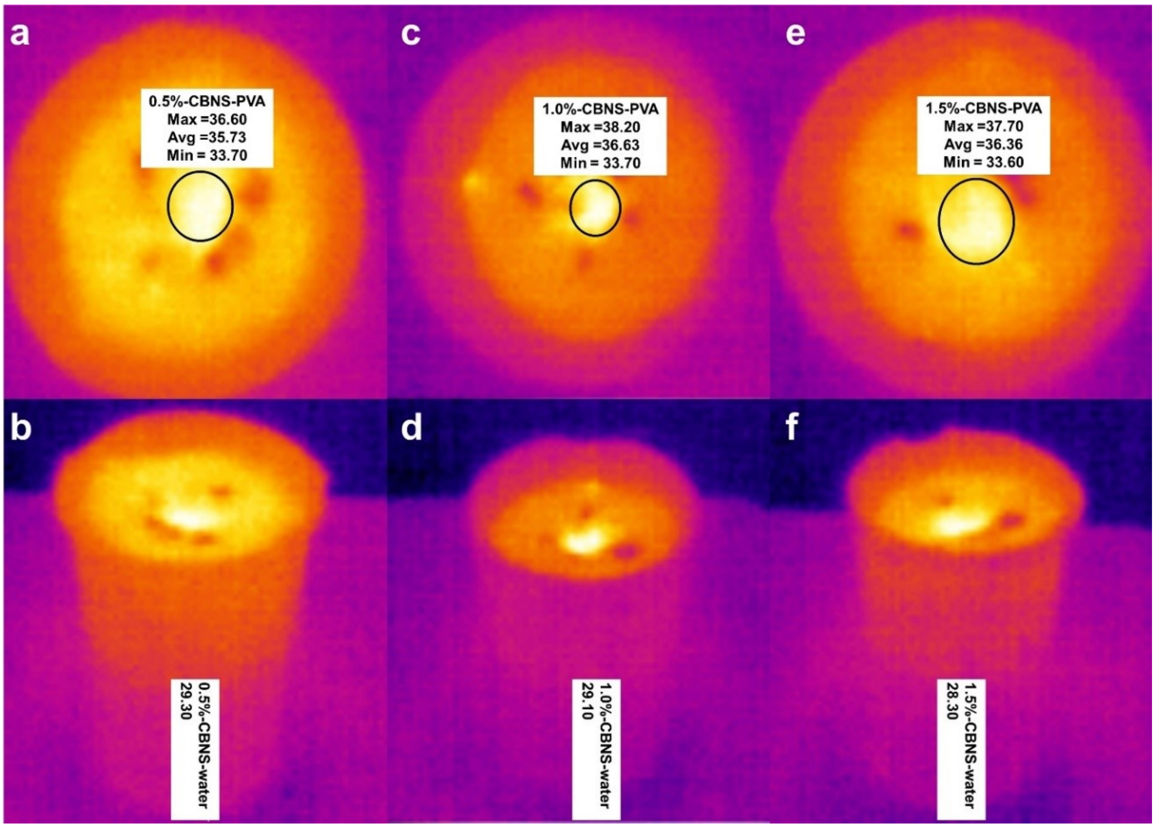

Fig. S14. Thermal infrared images of x-CBNS-PVA after 60 mins of SVG testing.

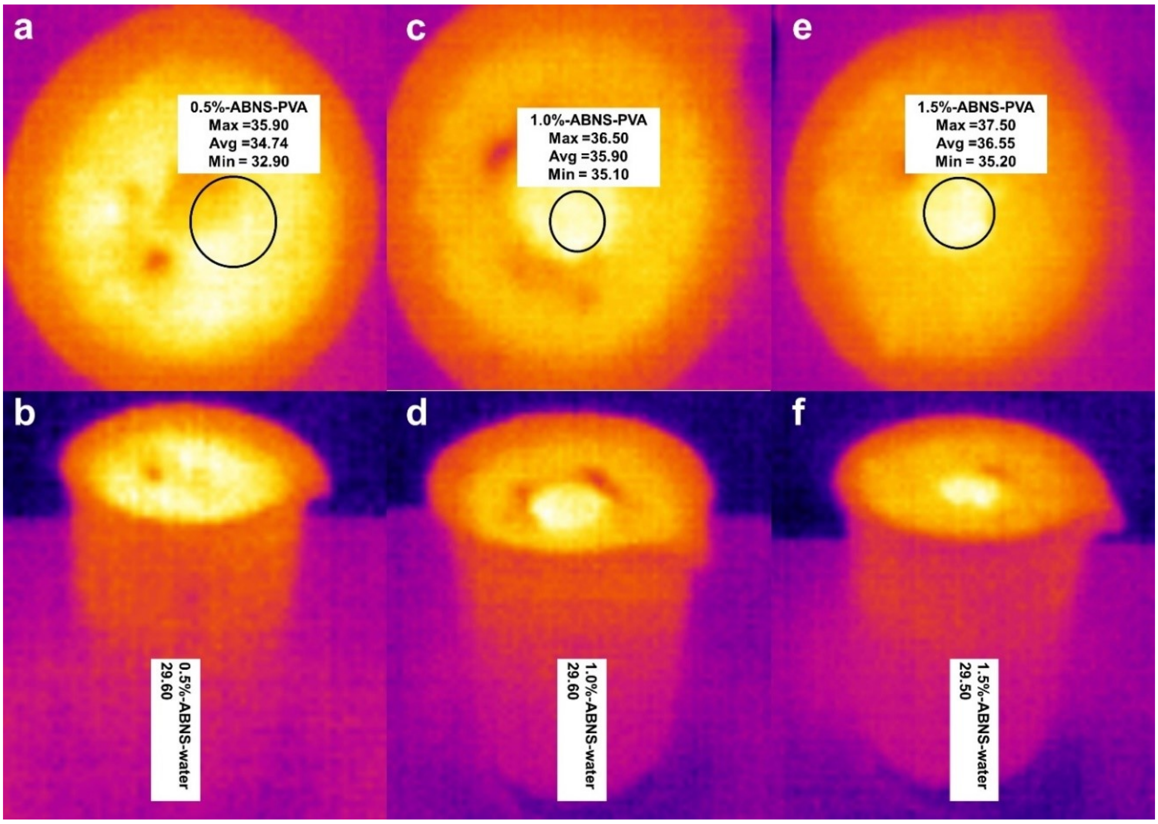

Fig. S15. Thermal infrared images of x-ABNS-PVA after 60 mins of SVG testing

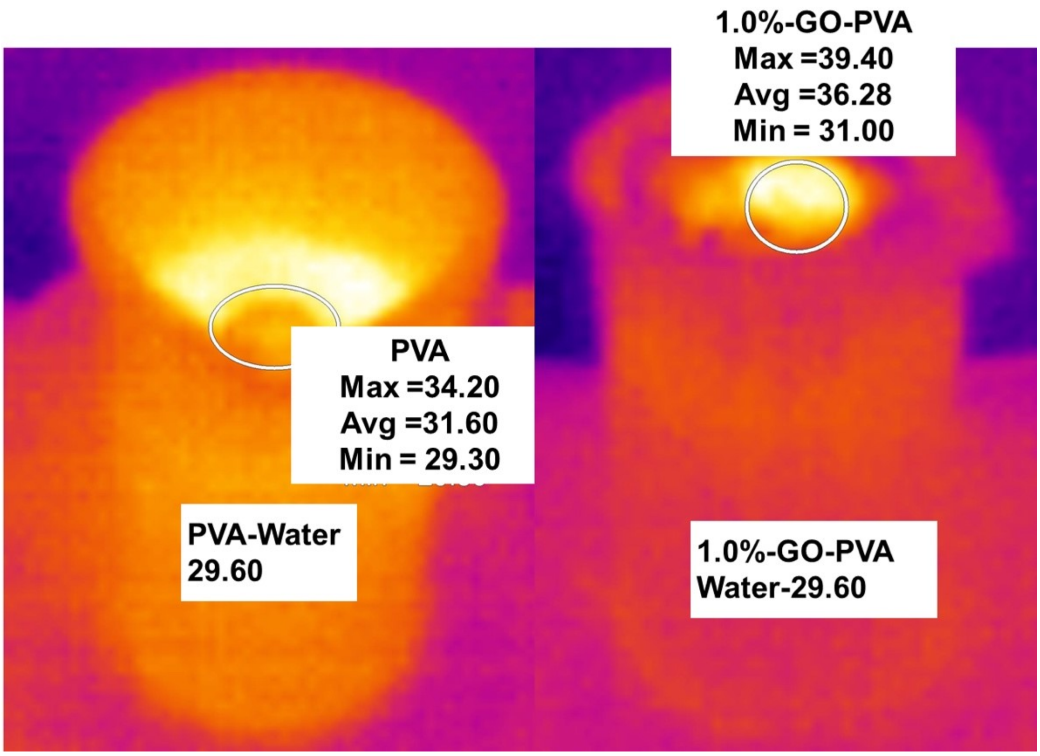

Fig. S16. Thermal infrared images of the pristine PVA and 1.0%-GO-PVA after 60 mins of SVG testing.

Table S2. The temperatures based on thermal infrared images of hydrogels at every 10 mins.

Hydrogels	**Temperature (°C)**						
	0 mins	**10 mins**	**20 mins**	**30 mins**	**40 mins**	**50 mins**	**60 mins**
0.5%-CBNS	23.10	35.40	36.00	36.10	36.40	36.10	36.60
Water-0.5%-CBNS	24.20	26.60	27.40	28.30	28.80	29.00	29.30
1.0%-CBNS	20.30	34.80	37.10	36.00	37.10	37.40	38.20
Water-1.0%-CBNS	23.60	24.10	26.10	26.20	27.50	28.70	29.10
1.5%-CBNS	20.20	33.90	35.80	35.70	36.20	36.80	37.70
Water-1.5%-CBNS	20.10	23.70	26.10	26.40	27.10	28.50	28.30
0.5%-ABNS	19.10	31.00	32.20	34.90	35.10	35.90	35.90
Water-0.5%-ABNS	21.90	23.60	26.70	27.60	28.10	29.60	29.60
1.0%-ABNS	22.80	33.60	34.10	35.00	35.90	36.40	36.50
Water-1.0%-ABNS	23.00	24.20	26.40	26.90	28.60	29.70	29.60
1.5%-ABNS	21.80	35.30	35.10	36.60	37.10	37.20	37.50
Water-1.5%-ABNS	22.40	24.10	25.60	27.00	28.40	28.60	29.50
PVA	21.00	32.30	32.50	34.60	33.70	34.00	34.20
Water-PVA	24.90	26.80	29.20	29.60	30.40	30.40	30.10

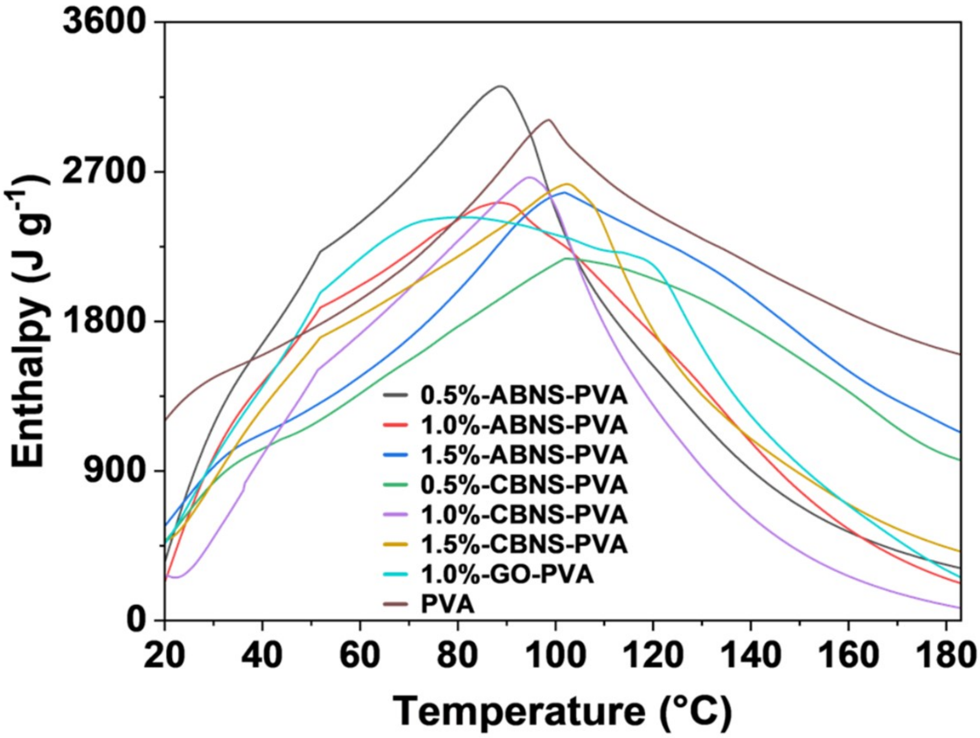

Fig. S17.The calculated equivalent water evaporation enthalpy at various temperatures using DSC data.

Table S3. An estimate of the equivalent water vaporisation enthalpy at the surface equilibrium temperature for the hydrogels.

Hydrogels	Equilibrium temperature	Equivalent evaporation enthalpy
	°C	$J\ g^{-1}$
0.5%-CBNS-PVA	35.73	951.87
1.0%-CBNS-PVA	36.60	845.11
1.5%-CBNS-PVA	36.30	1148.96
0.5%-ABNS-PVA	34.60	1438.60
1.0%-ABNS-PVA	35.90	1276.44
1.5%-ABNS-PVA	36.55	1071.47
1.0%-GO-PVA	36.28	1253.06
PVA	31.60	1483.95

Table S4. The comparison of evaporation rate, equivalent evaporation enthalpy and efficiency of all the hydrogels.

Hydrogels	**Evaporation rate**	**Equivalent evaporation enthalpy**	**Efficiency**
	kg m^{-2} h^{-1}	**J g^{-1}**	**%**
0.5%-CBNS-PVA	3.28	951.87	86.73
1.0%-CBNS-PVA	4.03	845.11	94.61
1.5%-CBNS-PVA	3.17	1148.96	101.17
0.5%-ABNS-PVA	2.71	1438.60	108.29
1.0%-ABNS -PVA	3.02	1276.44	107.08
1.5%-ABNS-PVA	3.19	1071.47	94.94
1.0%-GO-PVA	3.08	1253.06	107.21
PVA	1.31	1483.95	54.00

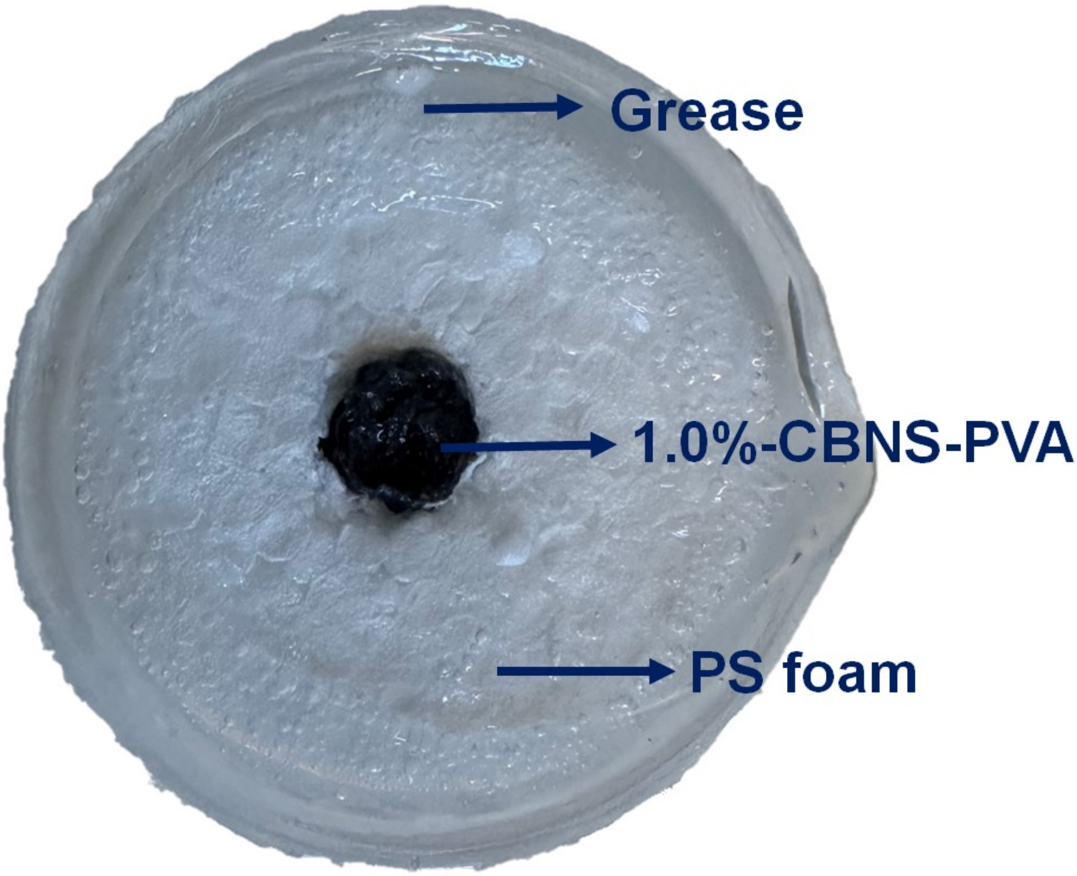

Fig. S18. The digital image of the 1.0%-CBNS-PVA surface after desalination for 14 days.

2. Comparison with state-of-the-art hydrogel evaporators

Table S6. The comparison among various functional sheets-based hydrogels.

Reference	Materials		Evaporation rate	Energy conversion efficiency
	Polymer	Others	kg m^{-2} h^{-1}	%
1	PVA	Nanoscale Surface Topography	2.6	91
2	PVA	$Ti_3C_2T_x$ MXene/r-GO	3.62	91
3	PVA	Konjac glucomannan (KGM), iron-based metal-organic framework (Fe-MOF)	3.2	90
4	PVA	trichloro(octadecyl)silane (OTS) patchy-surface hydrogel	4	93
5	PVA	Conducting polymer hollow spheres (CPHSs), superhydrophobic silica aerogel microparticles (SAMs)	1.83	82.2
6	PVA, polyacrylamide (PAM)	SA powder; Squid ink nanoparticles	2.3	71.38
7	PVA	Carboxylated multi-walled carbon nanotube (MWCNTs-COOH), hydrophobic PDMS as the top layer	1.34	85.71
8	PVA	Polypyrrole (PPy) and $FeCl_3.6H_2O$, 1H,1H,2H,2H-perfluoro octyl trichlorosilane (PFOTS) on the upper surface	1.68	94.7
9	PVA	Powdered activated carbon, glucose and yeast	1.611	95.15
10	PVA	A tree-inspired SSG system with Mxene ($Ti_3C_2T_x$)	2.71	90.7
11	PVA	Consists of internal gaps, micron channels and molecular meshes, polypyrrole (PPy)	3.2	94
12	PVA	r-GO, capillarity facilitated Water Transport	2.5	95
13	PVA and chitosan	Polypyrrole (PPy)	3.6	92
14	PVA and polystyrene sulfonate (PSS)	Activated carbon	3.86	92
15	polydimethylsiloxane (PDMS)	plasmonic Cu_7S_4-MoS_2-Au nanoparticles (CMA NPs)	3.824	96.6
16	PVA	titanium sesquioxide (Ti_2O_3)	3.6	90

17	PVA	molybdenum carbide (MoCx)	1.59	83.6
18	PVA	Graphene/graphene oxide composite nanosheet	1.44	86
19	PVA	Graphene and N-Methyl pyrrolidone	1.77	92
20	PVA	hydrogel-based ultrathin membrane (HUM)	2.4	75
21	PVA and chitosan (CS)	$Ti_3C_2T_x$ (MXene) and $La_{0.5}Sr_{0.5}CoO_3$(LSC)	2.73	92.3
22	PVA	Polydopamine (PDA)	2.94	94.5
23	PVA	Polypyrrole (PPy), micro-tree array	3.64	96
24	Nanofibrous PVA based membrane (NPM)	Polypyrrole (PPy) and graphene oxide (GO)	2.87	87.5
25	PVA and chitosan (CS)	Red Mud	2.185	90.74
26	PVA	Nanocarbon	1.67	86.8
27	PVA	Conjugated small molecule (DPP-2T)	2.6	89

3. Supporting references

1. Y. Guo, F. Zhao, X. Zhou, Z. Chen and G. Yu, *Nano Lett*, 2019, **19**, 2530-2536.
2. Y. Lu, D. Fan, Y. Wang, H. Xu, C. Lu and X. Yang, *ACS Nano*, 2021, **15**, 10366-10376.
3. Y. Guo, H. Lu, F. Zhao, X. Zhou, W. Shi and G. Yu, *Adv Mater*, 2020, **32**, e1907061.
4. Y. Guo, X. Zhao, F. Zhao, Z. Jiao, X. Zhou and G. Yu, *Energy & Environmental Science*, 2020, **13**, 2087-2095.
5. M. Tan, J. Wang, W. Song, J. Fang and X. Zhang, *Journal of Materials Chemistry A*, 2019, **7**, 1244-1251.
6. L. Zhao, J. Tian, Y. Liu, L. Xu, Y. Wang, X. Fei and Y. Li, *Environmental Science: Water Research & Technology*, 2020, **6**, 221-230.
7. H. Jian, Q. Qi, W. Wang and D. Yu, *Separation and Purification Technology*, 2021, **264**, 118459.
8. B. Wen, X. Zhang, Y. Yan, Y. Huang, S. Lin, Y. Zhu, Z. Wang, B. Zhou, S. Yang and J. Liu, *Desalination*, 2021, **516**, 115228.
9. X. Liang, X. Zhang, Q. Huang, H. Zhang, C. Liu and Y. Liu, *Solar Energy*, 2020, **208**, 778-786.
10. Z. Yu and P. Wu, *Advanced Materials Technologies*, 2020, **5**, 2000065.
11. F. Zhao, X. Zhou, Y. Shi, X. Qian, M. Alexander, X. Zhao, S. Mendez, R. Yang, L. Qu and G. Yu, *Nat Nanotechnol*, 2018, **13**, 489-495.
12. X. Zhou, F. Zhao, Y. Guo, Y. Zhang and G. Yu, *Energy & Environmental Science*, 2018, **11**, 1985-1992.
13. X. Zhou, F. Zhao, Y. Guo, B. Rosenberger and G. Yu, *Science Advances*, 2019, **5**, eaaw5484.
14. X. Zhou, Y. Guo, F. Zhao, W. Shi and G. Yu, *Advanced Materials*, 2020, **32**, 2007012.
15. H. Wang, R. Zhang, D. Yuan, S. Xu and L. Wang, *Advanced Functional Materials*, 2020, **30**, 2003995.
16. Y. Guo, X. Zhou, F. Zhao, J. Bae, B. Rosenberger and G. Yu, *ACS Nano*, 2019, **13**, 7913-7919.
17. F. Yu, X. Ming, Y. Xu, Z. Chen, D. Meng, H. Cheng, Z. Shi, P. Shen and X. Wang, *Advanced Materials Interfaces*, 2019, **6**, 1901168.
18. J. Tian, X. Huang and W. Wu, *Industrial & Engineering Chemistry Research*, 2020, **59**, 1135-1141.
19. W. Lei, S. Khan, L. Chen, N. Suzuki, C. Terashima, K. Liu, A. Fujishima and M. Liu, *Nano Research*, 2021, **14**, 1135-1140.
20. H. Lu, W. Shi, F. Zhao, W. Zhang, P. Zhang, C. Zhao and G. Yu, *Advanced Functional Materials*, 2021, **31**, 2101036.
21. D. Fan, Y. Lu, H. Zhang, H. Xu, C. Lu, Y. Tang and X. Yang, *Applied Catalysis B: Environmental*, 2021, **295**, 120285.
22. Z. Huang, J. Wei, Y. Wan, P. Li, J. Yu, J. Dong, S. Wang, S. Li and C.-S. Lee, *Small*, 2021, **17**, 2101487.
23. Y. Shi, O. Ilic, H. A. Atwater and J. R. Greer, *Nature Communications*, 2021, **12**, 2797.
24. S. Chen, Y. Liu, Y. Wang, K. Xu, X. Zhang, W. Zhong, G. Luo and M. Xing, *Chemical Engineering Journal*, 2021, **411**, 128042.
25. P. Wang, X. Wang, S. Chen, J. Zhang, X. Mu, Y. Chen, Z. Sun, A. Wei, Y. Tian, J. Zhou, X. Liang, L. Miao and N. Saito, *ACS Applied Materials & Interfaces*, 2021, **13**, 30556-30564.

26. Y. Li, W. Hong, H. Li, Z. Yan, S. Wang, X. Liu, B. Li, H. Jiang and X. Niu, *Desalination*, 2021, **511**, 115113.
27. Q. Zhao, Z. Huang, Y. Wan, J. Tan, C. Cao, S. Li and C.-S. Lee, *Journal of Materials Chemistry A*, 2021, **9**, 2104-2110.